

Distinct CCK-2 Receptor Conformations Associated with β -Arrestin-2 Recruitment or Phospholipase-C Activation Revealed by a Biased Antagonist

Rémi Magnan,[†] Chantal Escriet,[†] Véronique Gigoux,[†] Kavita De,[†] Pascal Clerc,[†] Fan Niu,[†] Joelle Azema,^{‡,⊥} Bernard Masri,^{§,⊥} Arnau Cordomi,[†] Michel Baltas,^{‡,⊥} Irina G. Tikhonova,^{*,||} and Daniel Fourmy^{*,†}

[†]EA 4552, Université de Toulouse 3, 31432 Toulouse, France

[‡]CNRS, LSPCMIB, UMR-5068, Toulouse, France

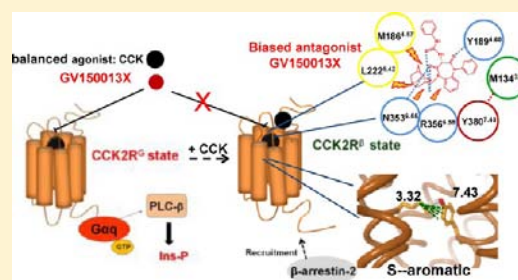
[§]INSERM U1037, Cancer Research Center of Toulouse, Toulouse, France

[⊥]Université de Toulouse 3, Toulouse, France

^{||}School of Pharmacy, Queen's University Belfast, Belfast BT9 7BL, United Kingdom

S Supporting Information

ABSTRACT: Seven-transmembrane receptors (7TMRs), also termed G protein-coupled receptors (GPCRs), form the largest class of cell surface membrane receptors, involving several hundred members in the human genome. Nearly 30% of marketed pharmacological agents target 7TMRs. 7TMRs adopt multiple conformations upon agonist binding. Biased agonists, in contrast to non-biased agonists, are believed to stabilize conformations preferentially activating either G-protein- or β -arrestin-dependent signaling pathways. However, proof that cognate conformations of receptors display structural differences within their binding site where biased agonism initiates, are still lacking. Here, we show that a non-biased agonist, cholecystokinin (CCK) induces conformational states of the CCK2R activating Gq-protein-dependent pathway (CCK2R^G) or recruiting β -arrestin2 (CCK2R ^{β}) that are pharmacologically and structurally distinct. Two structurally unrelated antagonists competitively inhibited both pathways. A third ligand (GV150013X) acted as a high affinity competitive antagonist on CCK2R^G but was nearly inefficient as inhibitor of CCK2R ^{β} . Several structural elements on both GV150013X and in CCK2R binding cavity, which hinder binding of GV150013X only to the CCK2R ^{β} were identified. At last, proximity between two conserved amino acids from transmembrane helices 3 and 7 interacting through sulfur–aromatic interaction was shown to be crucial for selective stabilization of the CCK2R ^{β} state. These data establish structural evidence for distinct conformations of a 7TMR associated with β -arrestin-2 recruitment or G-protein coupling and validate relevance of the design of biased ligands able to selectively target each functional conformation of 7TMRs.



INTRODUCTION

Seven-transmembrane receptors (7TMRs), also termed G protein-coupled receptors (GPCRs), form the largest class of cell surface membrane receptors, involving several hundred members in the human genome. Near 30% of marketed pharmacological agents target 7TMRs.¹ Biological effects triggered by 7TMRs result from the activation of both G protein-dependent and G protein-independent intracellular signaling pathways.²

The G protein-independent activation pathway often involves the recruitment of β -arrestins.^{3,4} In general, β -arrestin recruitment is preceded by receptor phosphorylation by 7TMRs kinases (G-protein coupled receptor kinases, abbreviated GRK) that selectively phosphorylate serine/threonine residues of agonist-activated 7TMRs.⁵ 7TMR-bound arrestins have been implicated in the activation of a number of signaling proteins such as the MAP kinase cascade (c-RAF-1, ERK1/2, JNK3) or non-receptor tyrosine kinases (c-Src, Yes).⁴ β -arrestins also play

a central role in orchestrating 7TMR trafficking since β -arrestin-bound 7TMRs are rapidly targeted to the clathrin-coated pits, thereby promoting internalization of these receptors.⁶ Importantly, therapeutic agents have been shown to activate differentially G protein-dependent or β -arrestin-dependent signaling pathways.⁷ Such ligands, triggering biased signaling, were named biased ligands or functionally selective ligands.⁷

Understanding the mechanism of biased signaling can provide more specific and efficient new drugs. It is generally assumed that the phenomenon of biased signaling is an intrinsic property of a ligand–7TMR complex, whereby a 7TMR exists in several conformations, each of which being preferentially stabilized and activated by selective ligands.⁸ However, despite the recent release of several X-ray structures of agonist–7TMR

Received: September 4, 2012

Published: January 16, 2013

complexes^{9–12} and biophysical and biochemical studies^{13–16} showing that different biased ligands induce or stabilize distinct conformations, experimental evidence directly linking distinct conformations of 7TMR to recruitment of β -arrestins or coupling to G proteins is still lacking. Furthermore, the mechanisms whereby biased agonism initiates in the binding site of 7TMR remain unknown.

In this context, we focused our study on the cholecystokinin-2 receptor, a member of family A 7TMRs, mediating central and peripheral effects of two important structurally related neuropeptides, cholecystokinin (CCK) and gastrin.¹⁷ We examined whether conformational states responsible for $G\alpha_q$ protein-dependent activation of phospholipase-C or recruitment of β -arrestins are distinguishable. For this purpose, we first compared pharmacologically the CCK-induced conformational state of the CCK2R recruiting β -arrestin-2 with that activating phospholipase-C, using structurally related and unrelated non-peptide ligands of the receptor. We discovered a non-peptide ligand (GV150013X), acting as a competitive antagonist on CCK2R inducing phospholipase-C activation but inefficient at inhibiting CCK2R inducing β -arrestin-2 recruitment to the CCK2R. We further identified structural elements on both GV150013X and the CCK2R, which hinder competitive binding of GV150013X to the orthosteric binding site of the CCK2R state recruiting β -arrestin-2. At last, we identified two interacting amino acids from helices 3 and 7 (M^{3.32} and Y^{7.43}) as key structural elements that govern stabilization of the CCK2R state recruiting β -arrestin-2. All together our data indicate that the non-biased agonist, CCK, induces distinct conformations of the CCK2R that activate phospholipase-C or recruit β -arrestin-2.

EXPERIMENTAL PROCEDURES

Materials. Sulfated [Thr²⁸,Nle³¹]-CCK 25–33 is referred to as CCK. ¹²⁵I-Sodium (2000 Ci/mmol) and [myo-3H]inositol (5 μ Ci/ml) were from GE Healthcare (Little Chalfont, Buckinghamshire, UK). Radio-iodinated CCK (1600–2000 Ci/mmol) is referred to as ¹²⁵I-CCK. Alexa Fluor 647-labeled CCK was obtained according to the procedure described recently for glucose insulinotropic polypeptide and is referred to as Alexa F 647-CCK.¹⁸ The following synthetic ligands of the CCK2R were used: PD135158,¹⁹ L365260,²⁰ and GV150013X.²¹ The cDNAs encoding CCK2R, green fluorescent protein (GFP)-tagged CCK2R and *Renilla* luciferase (Rluc)-fused CCK2R, were generated by subcloning respectively the CCK2R cDNA in pcDNAs/FTR (Invitrogen), pEGFP-N1 (BD Biosciences Clontech), or pRluc-N1(h) (Perkin-Elmer). Yellow fluorescent protein (YFP)-tagged β -arrestin-2 (termed β -arrestin-2-YFP) was a generous gift from Marc Caron (Duke University Medical Center, Durham, NC, USA). Red fluorescent protein (RFP)-tagged β -arrestin-2 (termed β -arrestin-2-RFP) was kindly given by Robert Lefkowitz (Duke University Medical Center). All mutant receptor cDNAs were constructed by oligonucleotide-directed mutagenesis (Quik Change site-directed mutagenesis kit, Stratagene, France) using human CCK2R cDNAs cloned in the pcDNAs/FRT vector as template. Cells used were HEK 293 cells stably expressing the CCK2R (Flp-In CCK2R-293, Flp-In system, Invitrogen) and HEK 293T cells transiently expressing proteins of interest. Transfections were performed using polyethylenimine (Polyscience). The different tagged CCK2Rs were pharmacologically characterized before use in the study. Binding experiments using ¹²⁵I-CCK indicated that wild-type CCK2R, GFP/YFP-tagged CCK2R, and Rluc-tagged CCK2R bound CCK with dissociation constant values (K_d) of 1.2 ± 0.2 , 1.1 ± 0.2 , and 0.9 ± 0.2 nM, respectively, and were expressed at similar levels. Inositol phosphate assays showed that they responded to CCK with similar potencies ($EC_{50} = 2.8 \pm 0.1$, 2.2 ± 0.2 , and 1.4 ± 0.4 nM, respectively) and exactly the same efficacy. Moreover, confocal microscopy analyses showed that Rluc-tagged CCK2R and wild-type CCK2R exhibited non-significantly different abilities to recruit YFP-tagged β -arrestin2

after stimulation by Alexa F 647 alone or in the presence of the antagonist GV150013X (not illustrated).

Receptor Binding Assay with ¹²⁵I-CCK. Cells grown overnight onto 10-cm culture dishes were transfected with 1 μ g/plate (except when mentioned) of vector containing the cDNA for the wild-type or mutated CCK2R-Rluc using polyethylenimine. Twenty-four hours later, cells were transferred to 24-well plates. Approximately 24 h later, binding assays were performed using ¹²⁵I-CCK according to the protocol previously described in detail.²² IC_{50} values for competitors (concentration inhibiting half of specific binding) were calculated using the nonlinear curve-fitting software GraphPad Prism (San Diego, CA). Mutation factors (F_{mut}) were calculated as $IC_{50}(\text{mutated CCK2R-Rluc})/IC_{50}(\text{wild-type CCK2R-Rluc})$.

Receptor Binding Assay by Flow Cytometry. Flp-InCCK2R-293 cells were incubated with Alexa F 647-CCK (0.1 μ M) alone or in the presence of competitors in DMEM/HEPES (20 mM) for 1 h at 37 °C in poly-L-lysine-coated 6-wells plates. Cell-associated fluorescence was determined using a BD FACSCalibur flow cytometer, with Flp-In 293 that does not express CCK2R as a negative control.

Inositol Phosphate Production Assay. Cells were prepared as for binding experiments and grown overnight in the presence of myo-[2-3H]inositol (2 μ Ci/mL, specific activity 10–25 Ci/mmol, Perkin-Elmer Life Sciences). Production of total inositol phosphates was determined as described previously.²²

Confocal Fluorescence Microscopy. Cells transiently transfected with appropriate plasmids were incubated with relevant agonists/antagonists and further observed by confocal fluorescence microscopy as described previously²³ using a Zeiss laser scanning microscope (LSM-510). For quantification, images of YFP and Alexa F 647 were collected using excitation lasers (488 and 633 nm) and double detection (windows: 504–633 nm and >650 nm) at the indicated times. The amount of β -arrestin-2-YFP (green) co-localizing with Alexa F 647-CCK-labeled CCK2R (red) was measured over time using Morpho Expert Software (Explora Nova, La Rochelle, France). Recruitment was expressed as the ratio between confocal co-localized β -arrestin-2-YFP/Alexa F 647-CCK-labeled CCK2R and Alexa F 647-CCK-labeled CCK2R. On average, 10–14 individually transfected cells were analyzed on 2 separate wells, representing a duplicate.

BRET Studies. β -Arrestin-2-YFP recruitment to ligand-occupied wild-type or mutated CCK2R-Rluc was assessed using a bioluminescence resonance energy transfer (BRET) assay in a 96-well format, as described in detail in the Supporting Information and previously in ref 23. For titration experiments, the acceptor/donor ratio was calculated as described previously.²⁴

Structural Modeling. Homology modeling of the CCK2R was conducted using the Prime module of the Schrödinger software (Prime 2.0, Schrödinger, LLC, New York, NY, USA) with the default settings. To mimic the experimental conditions, and the fact that the CCK2R^G state converted to the CCK2R ^{β} state upon CCK binding, we built the CCK2R^G state using the crystal structure of the nanobody-stabilized active form of the β_2 adrenergic receptor (PDB code: 3P0G) available at the time of our modeling study.²⁵ CCK was docked into this modeled CCK2R^G on the basis of our previous mutagenesis data,^{22,26–31} enabling refinement of the model. Docking of non-peptide ligands was performed using the Glide 5.6 module of the Schrödinger software and guided using constraints derived from results of the binding study in which we measured the effect of mutations within the binding cavity of the CCK2R on the affinity of the ligands (Table 1). The docking poses were reoptimized on the basis of the obtained binding data (Table 1) using the Induced-Fit module.³² All ligands were preprocessed with LigPrep at pH 7. The standard precision scoring function was used in Glide. To examine the dynamics of the complexes, we used the Dynamics module of MacroModel (Schrödinger, LLC). Electrostatics was set to distance-dependent function and dielectric constant of 4. The backbone hydrogen bonds of transmembrane helices were constrained to preserve the secondary structure. The biosystems were minimized within 500 steps and subjected to 20 ns molecular dynamics with a default setting. OPLS2005 force field was used for all calculations. Maestro

Table 1. Effect on Mutations within the Orthosteric Binding Site of the CCK2R on Affinity of Antagonists L365260, GV150013X, and GV-CH3^a

	GV150013X		antagonists L365260		GV-CH3	
	IC ₅₀ ± SEM (nM)	F _{mut}	IC ₅₀ ± SEM (nM)	F _{mut}	IC ₅₀ ± SEM (nM)	F _{mut}
WT-CCK2R	3.75 ± 0.14	1.0	8.7 ± 0.4	1.0	115 ± 25	1.0
T111A ^{2.61} -CCK2R	1.52 ± 0.39***	0.4	52.8 ± 9.5**	6.1	239 ± 49*	2.1
M134A ^{3.32} -CCK2R	27.7 ± 6.6*	7.3	91.8 ± 45.0*	10.6*	ND	ND
Y189A ^{4.60} -CCK2R	26.6 ± 2.6**	7.0	5.2 ± 0.7	0.6	437 ± 75*	3.8
L222A ^{5.42} -CCK2R	1.76 ± 0.59**	0.5	4.3 ± 1.0**	0.5	ND	ND
L223A ^{5.43} -CCK2R	15.7 ± 2.4***	4.2	28.7 ± 7.4**	3.3	ND	ND
F227A ^{5.49} -CCK2R	3.7 ± 0.2	1.0	22.5 ± 1.8***	2.6	ND	ND
W346A ^{6.48} -CCK2R	4.0 ± 0.8	1.1	6.9 ± 1.2	0.8	ND	ND
N353A ^{6.55} -CCK2R	15.4 ± 2.5**	4.1	45.9 ± 14.4**	5.3**	ND	ND
R356A ^{6.58} -CCK2R	14.2 ± 2.9**	3.8	4.2 ± 0.8	0.5	721 ± 95**	6.3
H376A ^{7.39} -CCK2R	10.5 ± 0.3***	2.8	7.8 ± 0.9	0.9	ND	ND
Y380A ^{7.43} -CCK2R	14.4 ± 1.5***	3.1	25.1 ± 8.6**	2.9	ND	ND

^aBinding experiments were performed as indicated in the Experimental Procedures section on HEK 293T cells transiently expressing wild-type or mutated CCK2R-Rluc. Results are given as IC₅₀ (concentration of antagonists inhibiting 50% of ¹²⁵I-CCK specific binding) and mutation factors F_{mut}, which were calculated as IC₅₀(mutated CCK2R-Rluc)/IC₅₀(wild-type CCK2R-Rluc). IC₅₀ values are means ± SEM from three or four separate determinations. Asterisks indicate *p* values giving significance of IC₅₀ shifts for mutants relative to wild-type CCK2R: * 0.01 < *p* < 0.05; ** 0.001 < *p* < 0.01; *** *p* < 0.001. ND = affinity was not determined.

Schrödinger utilities (Schrödinger, LLC) and VMD scripts³³ were used for the trajectories analyses.

Statistical Analyses. Unpaired *t* test (Prism GraphPad software) was used. Values for CCK2R mutants (binding, inositol phosphate production, β -arrestin2 recruitment) were compared to that of the wild-type CCK2R. In figures and tables, degree of confidence is indicated by asterisks as follows: * 0.01 < *p* < 0.05; ** 0.001 < *p* < 0.01; *** *p* < 0.001.

RESULTS

The CCK2R ^{β} State Recruiting β -Arrestin-2 Is Pharmacologically Distinct from the CCK2R^G State Activating Phospholipase-C. Binding of cholecystokinin (CCK) to the CCK2R (Figure 1a) activates a G α q signaling pathway, namely phospholipase-C activation,³⁴ which we monitored using the inositol phosphate assay in HEK 293 cells (Figure 1b). The conformational state of the CCK2R responsible for G α q-dependent stimulation of phospholipase-C upon CCK stimulation was named CCK2R^G (Figure 1b). Moreover, under CCK stimulation, β -arrestin-2 is rapidly recruited to the CCK2R. This recruitment was followed by observing translocation of cytoplasmic β -arrestin-2-GFP to activated CCK2R with fluorescent CCK, and by measuring specific increase of BRET signal between CCK2R-Rluc and β -arrestin-2-YFP.²³ The state of the CCK2R recruiting β -arrestin-2 upon CCK stimulation was named CCK2R ^{β} (Figure 1b).

To initiate molecular and structural comparison of the CCK-induced CCK2R ^{β} and CCK2R^G states, we investigated whether the binding cavity of the two functional states, involving residues from transmembrane helices (Figure 1a and ref 22) could show differences. Thus, the ability of three standard molecules (PD135158, L365260, and GV150013X) (Figure 1c) to inhibit CCK-stimulated production of inositol phosphates or β -arrestin-2 recruitment was assessed in HEK 293 cells. As shown in Figure 2a–d, CCK-stimulated inositol phosphate production was dose-dependently inhibited by PD135158, L365260, and GV150013X. These results are in agreement with binding data indicating that ¹²⁵I-CCK binding to HEK cells expressing the CCK2R was dose-dependently and fully inhibited by PD135158, L365260, and GV150013X with

IC₅₀ = 4.06, 9.19, and 3.60 nM, respectively (Supplementary Fig. 1). On the other hand, β -arrestin-2 recruitment to the CCK2R was dose-dependently inhibited by PD135158 and L365260 but not by GV150013X, suggesting that GV150013X, despite its structural similarity with L365260, is unable to compete with CCK for the CCK2R ^{β} state (Figure 2e–h).

We further ensured that L365260 and GV150013X, which are structurally related compounds, and PD135158, a pseudopeptidic ligand (Figure 1c), bind to the CCK2R orthosteric binding site in a competitive manner by analyzing the data using a Schild plot. As illustrated on Figure 3a, CCK dose–response curves of inositol phosphate production were right shifted in the presence of increasing concentration of PD135158, L365260, or GV150013X and reached the same maximal response. This indicates that all three non-peptide ligands inhibited phospholipase-C activation competitively. CCK dose–response curves of BRET were similarly right shifted in the presence of increasing concentration of PD135158 or L365260 and not in the presence of GV150013X (Figure 3b). Thus, unlike GV150013X, both L365260 and PD135158 inhibit β -arrestin-2 recruitment through binding to the orthosteric binding site of the CCK2R ^{β} state. Comparison of dose–response curves indicates that the potency of CCK (EC₅₀) in BRET experiments (10.6 ± 1.9 nM) was lower than that of CCK alone in inositol phosphate assays (1.4 ± 0.37 nM). This suggested possible switch of pathways from stimulation of phospholipase-C through high affinity CCK binding sites to β -arrestin2 recruitment through low affinity binding sites.

Since CCK2R-induced β -arrestin-2 recruitment is a molecular event preceding CCK2R internalization and trafficking,²³ we then investigated the effects of non-peptidic ligands on CCK-stimulated internalization of the CCK2R. GFP-tagged CCK2R was located at the cell membrane and was internalized under CCK stimulation (Figure 4a,b). PD135158 or L365260 fully inhibited CCK-induced internalization of GFP-tagged CCK2R (Figure 4c,d). Remarkably, GV150013X, which did not stimulate internalization by itself, only weakly inhibited internalization of GFP-tagged CCK2R (Figure 4f,g). We next investigated whether the absence of inhibitory effect of GV150013X

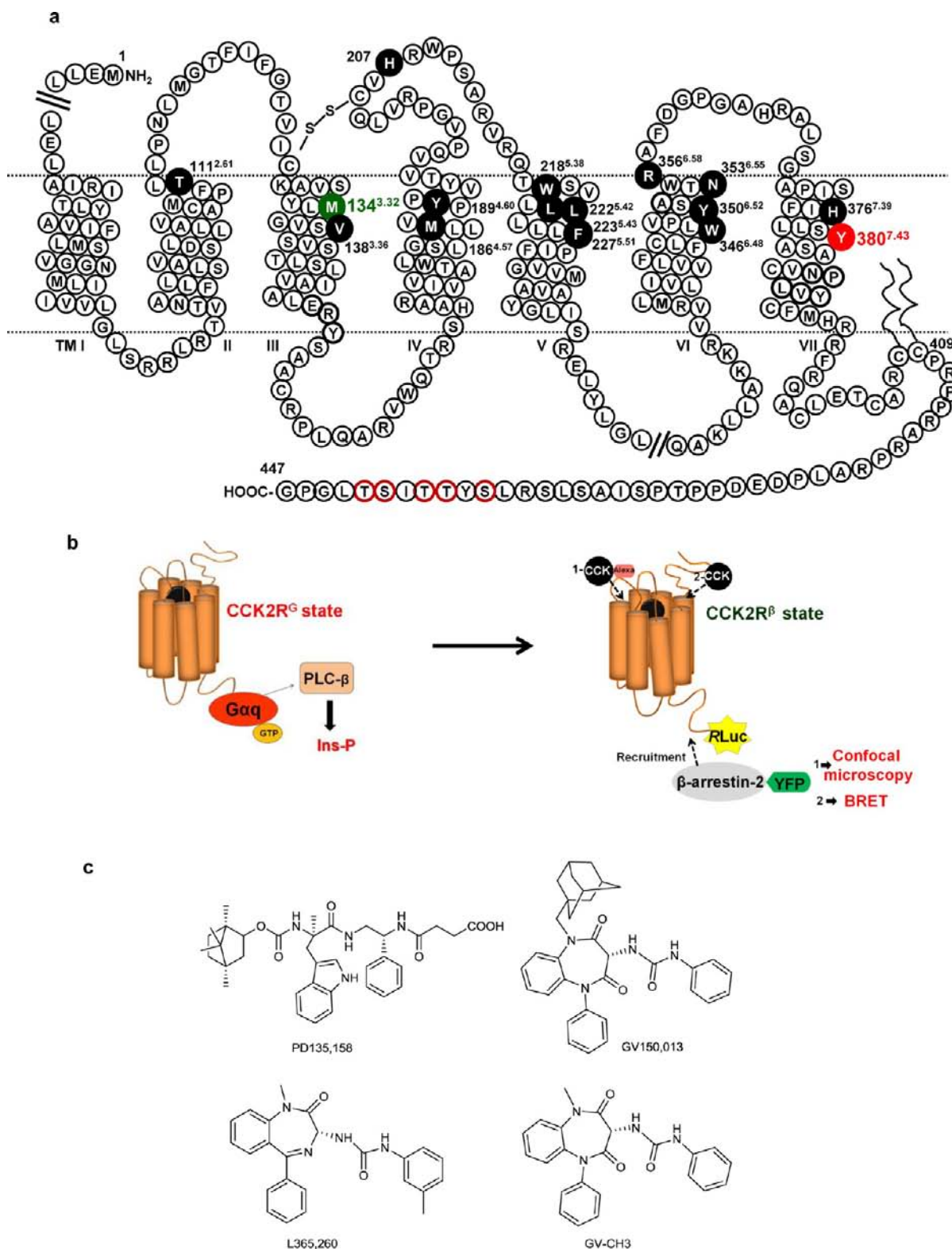


Figure 1. Representation of CCK2R and assays used to study states signaling through $G\alpha_q$ coupling or recruiting β -arrestin-2. (a) Serpentine representation of the human CCK2R. Amino acids previously identified as participating in the orthosteric binding site²⁸ and/or activation site^{29,34,66} (black full circles), as well as the endocytosis motif in the C-terminal region²³ (black letters in red circles), are depicted and double-numbered (main number, regular numbering for proteins; superscript numbers, Ballesteros–Weinstein numbering). (b) Diagrams illustrating the principle of assay for the CCK2R^G state signaling through $G\alpha_q$ coupling or the CCK2R ^{β} state recruiting β -arrestin-2 by measurement of inositol phosphate production or BRET, respectively. (c) Chemical structures of CCK2R non-peptide ligands used in the study.

on CCK2R ^{β} state (whereas this compound fully competed with ¹²⁵I-CCK in binding experiments, Supplementary Fig. 1) could

be due to the presence of a population of CCK2R binding sites recognizing CCK, albeit with a low affinity, but not recognizing

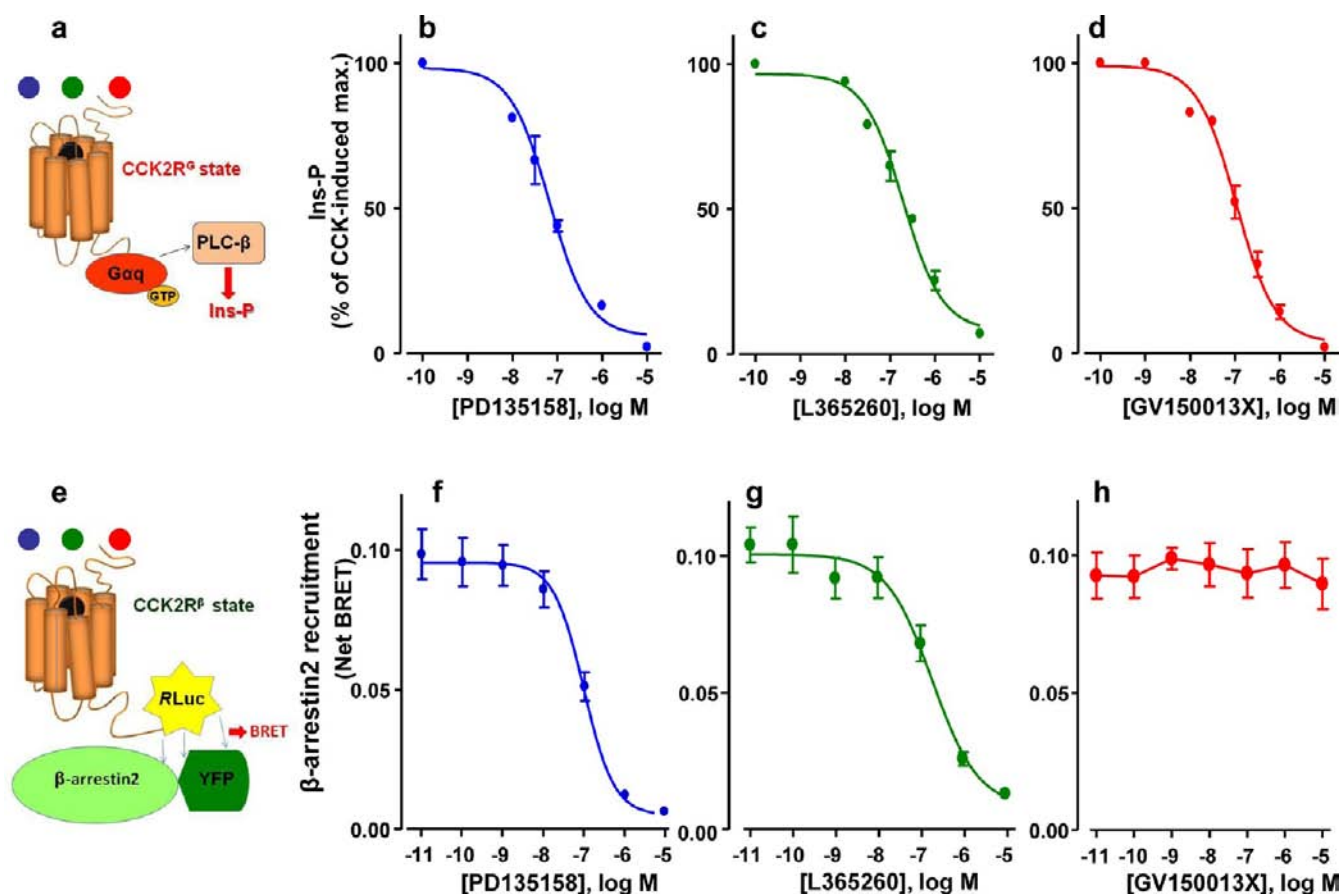


Figure 2. Effect of antagonists showing inability of GV150013X to inhibit CCK-induced β -arrestin-2 recruitment to the CCK2R. (a–d) Inositol phosphate (Ins-P) accumulation upon stimulation for 60 min with 10 nM CCK alone or in the presence of increasing concentrations of PD135158, L365260, or GV150013X. Experiments were carried out with Flp-InTM CCK2R-293 cells expressing the wild-type CCK2R. Results are expressed as the percent of inositol phosphate production achieved with 10 nM CCK alone. (e–h) BRET between β -arrestin-2 and CCK2R upon stimulation for 300 s with 100 nM CCK in the absence or in the presence of increasing concentrations of PD135158, L365260, or GV150013X added at the same time, before BRET measurements. Experiments were carried out with HEK 293T cells transiently expressing the wild-type CCK2R-Rluc and β -arrestin-2-YFP. Results are expressed as net BRET as described in the Experimental Procedures. Data are the mean \pm SEM of three or four independent experiments, each determination being performed in triplicate.

GV150013X. For this purpose, we performed confocal microscopy observations of HEK cells incubated with Alexa F 647-CCK in the presence of GV150013X at a saturating concentration. As shown on Figure 4g, fluorescent CCK still abundantly internalized in the presence of GV150013X. We next performed binding experiments using Alexa F 647-CCK in order to probe such low affinity binding sites. Interestingly, these binding experiments enabled identification of a fraction of CCK binding sites (>30% of total binding sites) which were not occupied by GV150013X even at 10 μ M concentration (Figure 5), thus suggesting a relationship between the fraction of labeled CCK2R in the presence of GV150013X and internalization (Figure 4g). Hence, CCK2R binding sites presenting a low affinity for CCK and unable to bind GV150013X are identified in HEK cells. These CCK2R binding sites likely correspond to CCK2R^β state recruiting β -arrestin2.

This first set of pharmacological results allows us to propose the view that CCK-stimulated formation of the CCK2R^G state stimulating phospholipase-C is prevented in a competitive fashion by the non-peptide ligands PD135158, L365260, or GV150013X. The CCK2R^G state is converted to the CCK2R^β state recruiting β -arrestin-2 upon CCK binding, probably GRK action, and subsequently undergoes internalization. The formation of CCK2R^β- β -arrestin2 complex upon CCK stimulation is

inhibited by PD135158 or L365260 and not by GV150013X. This striking result led us to investigate the molecular basis for the absence of inhibitory effect of GV150013X on CCK-induced formation of CCK2R^β state recruiting β -arrestin-2.

Structural Basis for Distinct Behavior of Benzodiazepine-like Antagonists on the CCK2R^β State Recruiting β -Arrestin-2 or the CCK2R^G State Activating Phospholipase-C. At this point, we focused our study on the two benzodiazepine-like ligands, GV150013X, with a bulky adamantane group, and L365260, with a methyl group at the similar position, as shown in Figure 1c. Comparison of the two structures led us to hypothesize that the adamantane ring may hinder competitive binding of GV150013X to the CCK2R^β state and not to the CCK2R^G state. Following this hypothesis, we postulated that exchange of amino acids in contact with the adamantane group within the orthosteric binding site of the CCK2R by a residue having a smaller side chain or chemical substitution of adamantane by a smaller group would restore ligand binding at the CCK2R^β state and therefore, inhibition of CCK-stimulated recruitment of β -arrestin-2.

For this purpose, the CCK2R^G state of CCK2R was homology modeled using the crystal structure of the nanobody-stabilized active form of the β 2 adrenergic receptor.²⁵ The model was further refined on the basis of the mutagenesis data used to

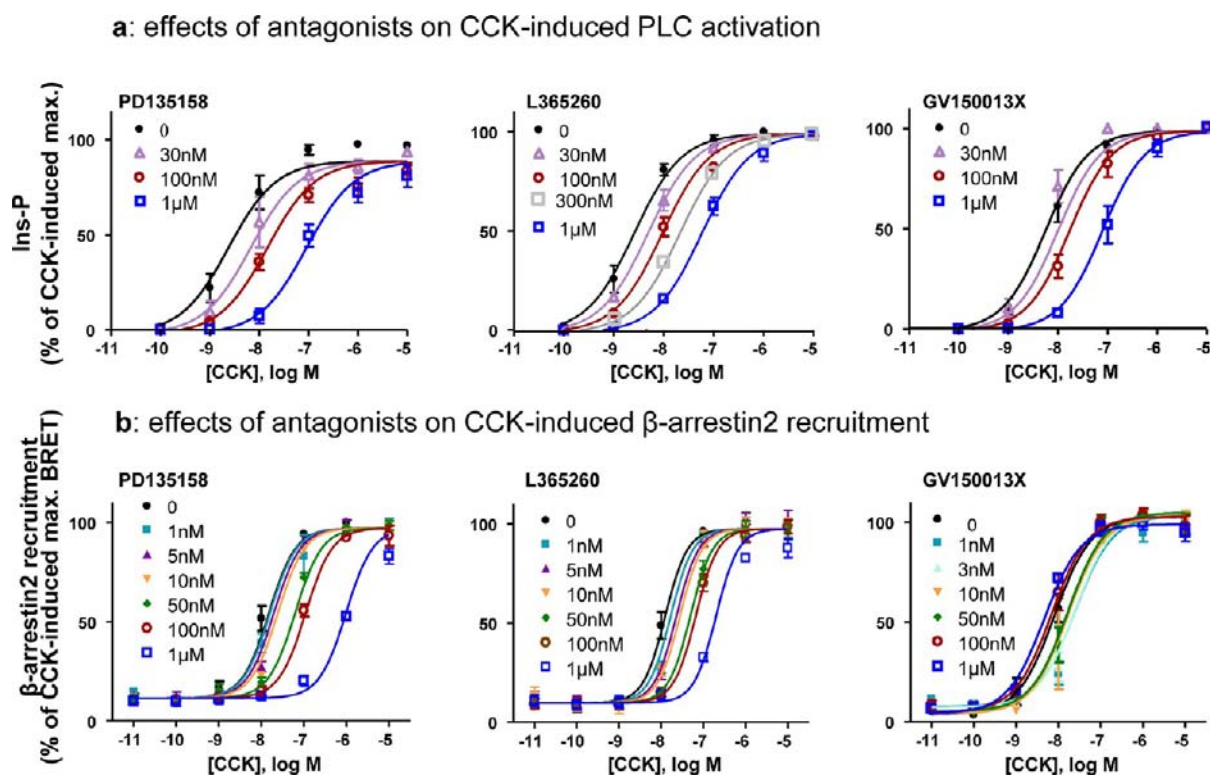


Figure 3. Analysis of antagonist effects using Schild plot shows that GV150013X interacts competitively with CCK2R^G state stimulating phospholipase-C but could not competitively interact with the CCK2R ^{β} state recruiting β -arrestin-2. (a) Effect of antagonists on CCK-induced inositol phosphate production. Flp-InTM CCK2R-293 cells expressing the wild-type CCK2R were stimulated for 60 min with increasing concentrations of CCK alone (indicated on x axis) or in combination with PD135158, L365260, or GV150013X at indicated concentrations. Results are expressed as the percent of inositol phosphate production achieved with CCK alone and are the mean \pm SEM of four independent experiments, each determination being performed in triplicate. $pA_2 = 7.82 \pm 0.23$, 7.46 ± 0.07 , and 7.38 ± 0.16 were calculated using GraphPad Prism software for PD135158, L365260, and GV150013X, respectively. (b) Effect of antagonists on BRET between β -arrestin-2 and CCK2R. HEK 293T cells transiently expressing wild-type CCK2R-Rluc and β -arrestin-2-YFP were stimulated for 300 s with increasing concentrations of CCK alone (indicated on x axis) or in combination with PD135158, L365260, or GV150013X at indicated concentrations before BRET measurements. Results are expressed as net BRET as previously described.²³ Data are the mean \pm SEM of 4–6 independent experiments, each determination being performed in triplicate. $pA_2 = 7.79 \pm 0.08$ and 8.15 ± 0.04 were calculated using GraphPad Prism software for PD135158 and L365260, respectively.

validate the key residues interacting with CCK in our previous works^{22,28,29,31} (Supplementary Fig. 2). We then docked GV150013X and L365260 to the refined model of the CCK2R^G state. Docking experiments predicted most probable binding poses of GV150013X and L365260 that are likely distinct (Figure 6). More precisely, molecular docking suggested that GV150013X binds between helices 3–6 and is surrounded by Y189^{4,60}, N353^{6,55}, and R356^{6,58} likely through hydrogen bonds and by M134^{3,32}, M186^{4,57}, L223^{5,43}, W346^{6,48}, H376^{7,39}, and Y380^{7,43} via hydrophobic contacts. On the other hand, docking suggested that L365260 binds between helices 2–3 and 6–7, establishing hydrogen bonds with T111^{2,61}, Y380^{7,43}, and N353^{6,55} and hydrophobic interactions with M134^{3,32}, L223^{5,43}, F227^{5,47}, and Y380^{7,43}.

Since the docking experiments predicted distinct poses of L365260 and GV150013X into the orthosteric binding site of the CCK2R, we experimentally verified whether the mutation of amino acids of the binding cavity could support (or refute) the docking data. Binding results with CCK2R mutants (Table 1) indicated that alanine mutations of residues Y189^{4,60}, R356^{6,58}, or H376^{7,39} stronger affected the affinity of GV150013X than that of L365260. In contrast, alanine mutation of residues T111^{2,61} or F227^{5,47} stronger affected the binding affinity of L365260 than that of GV150013X. At last, mutation of residues M134^{3,32}, L223^{5,43}, N353^{6,55}, or Y380^{7,43} to alanine almost equally affected the

binding affinity of both ligands for the CCK2R. Thus, results from site-directed mutagenesis and molecular docking agree with the view of a distinct ligand positioning within the binding pocket of the CCK2R^G, though, there is significant overlapping (Supplementary Fig. 3).

From the proposed GV150013X binding pose, we hypothesized that amino acids M186^{4,57}, L222^{5,42}, L223^{5,43}, N353^{6,55}, and R356^{6,58}, which were close to the adamantane group of GV150013X in the CCK2R^G binding site, could hinder binding of the antagonist to the CCK2R ^{β} state recruiting β -arrestin-2. To test this hypothesis we mutated these residues to alanine and measured β -arrestin-2 recruitment by BRET. Remarkably, GV150013X dose-dependently inhibited CCK-stimulated β -arrestin-2 recruitment to mutants M186A^{4,57} and L222A^{5,42}, whereas it was almost ineffective in inhibition of β -arrestin-2 recruitment to the wild-type CCK2R (Figure 7a and Table 2). On the other hand, GV150013X dose-dependently inhibited CCK-induced inositol phosphate production with an identical high potency on mutants M186A^{4,57} and L222A^{5,42} and on wild-type CCK2R (Figure 7b and Table 2). Control experiments indicate that mutants M186A^{4,57} and L222A^{5,42} recruit β -arrestin-2 or stimulated inositol phosphate in response to CCK stimulation with the same efficacy as the wild-type CCK2R indicating that the two mutants were fully converted to either CCK2R ^{β} or CCK2R^G states following CCK stimulation (Supplementary Fig. 4).

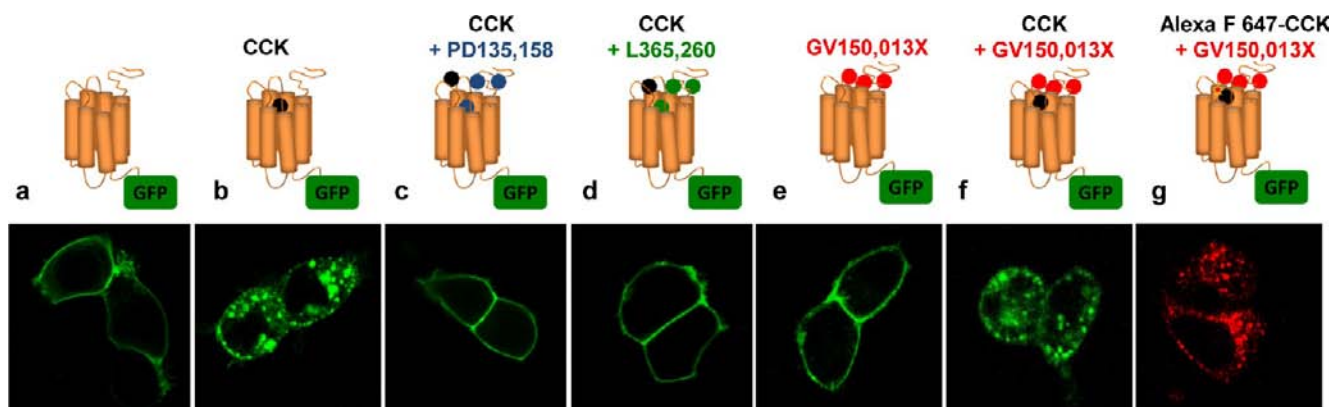


Figure 4. Absence of competitive inhibition of CCK-stimulated internalization of CCK2R by GV150013X. Confocal microscopy images of HEK 293T cells transfected with CCK2R-GFP: (a) Cells were not stimulated with CCK and cells were incubated at 37 °C with CCK (100 nM) alone for 30 min (b) or with CCK (100 nM) plus PD135158 (c) or L365260 (d). In (e) cells were incubated for 30 min with GV150013X alone (1 μM), and in (f) with CCK (100 nM) plus GV150013X (10 μM). In (g) cells were incubated for 30 min with Alexa F 647-CCK (0.1 μM) in the presence of GV150013X (10 μM). Antagonists were added at the same time as CCK. Images are representative of at least 10 separate observations (cell number, $n > 5$) on two different batches of transfected cells ($N = 2$).

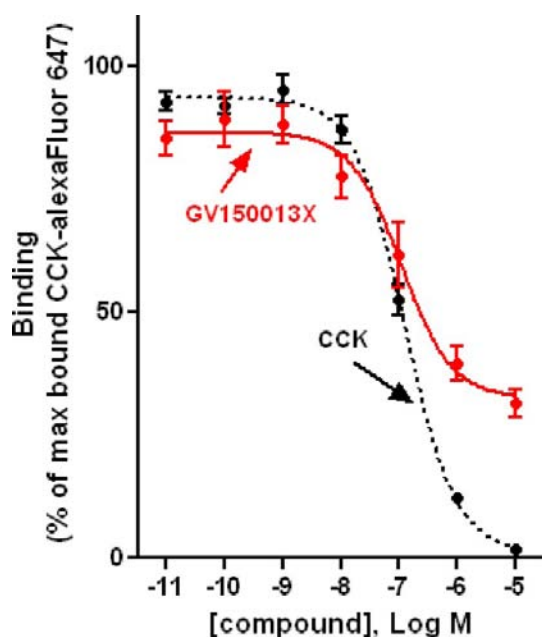


Figure 5. Evidence for the existence of a low-affinity CCK binding site which does not recognize GV150013X. Inhibition of binding was carried out by incubating Alexa F 647-CCK (0.1 μM) in the presence of increasing concentrations of CCK or GV150013X for 60 min, as described in the Experimental Procedures. Specific binding was assayed by flow cytometry, and results are expressed as the percent of maximal specific binding in the absence of competitor, and are the mean \pm SEM of three or four experiments.

Furthermore, we synthesized the analogue of GV150013X (abbreviated as GV-CH₃) in which the adamantane group was substituted by a methyl group for further assessment of the adamantane role in preventing β -arrestin-2 recruitment. We found that unlike GV150013X, GV-CH₃ dose-dependently inhibits CCK-stimulated β -arrestin-2 recruitment to the wild-type CCK2R, although with a low potency (Figure 7c and Table 2). Interestingly, antagonist potency of GV-CH₃ was increased on mutants M186A^{4,57} and L222A^{5,42} relative to wild-type CCK2R (Figure 7, Supplementary Fig. 5, and Table 2). In contrast, GV-CH₃ dose-dependently inhibited CCK-induced inositol phosphate production with an identical potency on mutants M186A^{4,57} and

L222A^{5,42} or on wild-type CCK2R and this potency was about 50, 85, and 113 fold lower than that of GV150013X, respectively (Figure 7 and Supplementary Fig. 5 and Table 2). GV150013X at 10 μM also inhibited CCK-stimulated β -arrestin-2 recruitment to mutants N353A^{6,55} and R356A^{6,58} but not to L222A^{5,43} (Supplementary Fig. 6). Note that the activity of L365260 and PD135158 on the mutants was unchanged compared to the wild-type CCK2R (Supplementary Fig. 6).

To summarize, pharmacological data show that adamantane substitution by methyl group in GV150013X enables the antagonist to interact with CCK2R ^{β} state whereas this chemical change dramatically decreases the potency of the antagonist on CCK2R ^{γ} state (opposite effects caused by chemical substitution). Furthermore, mutation of residues M186^{4,57} and L222^{5,42} to alanine in the CCK2R enables GV150013X to interact with CCK2R ^{β} state and also increases the potency of GV-CH₃ on CCK2R ^{β} state whereas the mutation of these residues do not affect significantly potency of the antagonists on CCK2R ^{γ} state.

Given that pharmacological studies suggested that substitution of adamantane in GV150013X by methyl enables GV-CH₃ to bind to the CCK2R ^{β} state, the binding pose of GV-CH₃ in the CCK2R was explored by molecular docking and binding experiments with the selected CCK2R mutants, involving T111^{2,61}, M134^{3,32}, Y189^{4,60} and R356^{6,58} (Table 1). Our data suggest that the position of GV-CH₃ in the CCK2R binding site partially overlaps that of GV150013X, in particular, the diazepinedione moiety likely interacts with residues R356^{6,58} and Y189^{4,60} as shown on Figure 6c. However, GV-CH₃ seats deep in the orthosteric binding cavity and the 1-phenylurea moiety, similar to the 1-phenylurea moiety of L365260, interacts with helices 3 and 6 and is close to T111^{2,61}. This pose of GV-CH₃ into the binding site may explain the low potency of GV-CH₃ for the CCK2R ^{γ} state as well as its low potency as inhibitor of β -arrestin recruitment on CCK2R ^{β} state (Table 2).

Therefore, steric hindrance between the adamantane group of GV150013X and residues M186^{4,57}, L222^{5,42} of the CCK2R (and to less extent, N353^{6,55} and R356^{6,58}) most likely explains in part inability of GV150013X to competitively interact with the CCK2R ^{β} state. Interestingly, the fact that this steric hindrance was observed with the CCK2R ^{β} state recruiting β -arrestin-2 and not with the CCK2R ^{γ} state stimulating phospholipase-C suggests that transition of the CCK2R from the CCK2R ^{γ} state to the CCK2R ^{β}

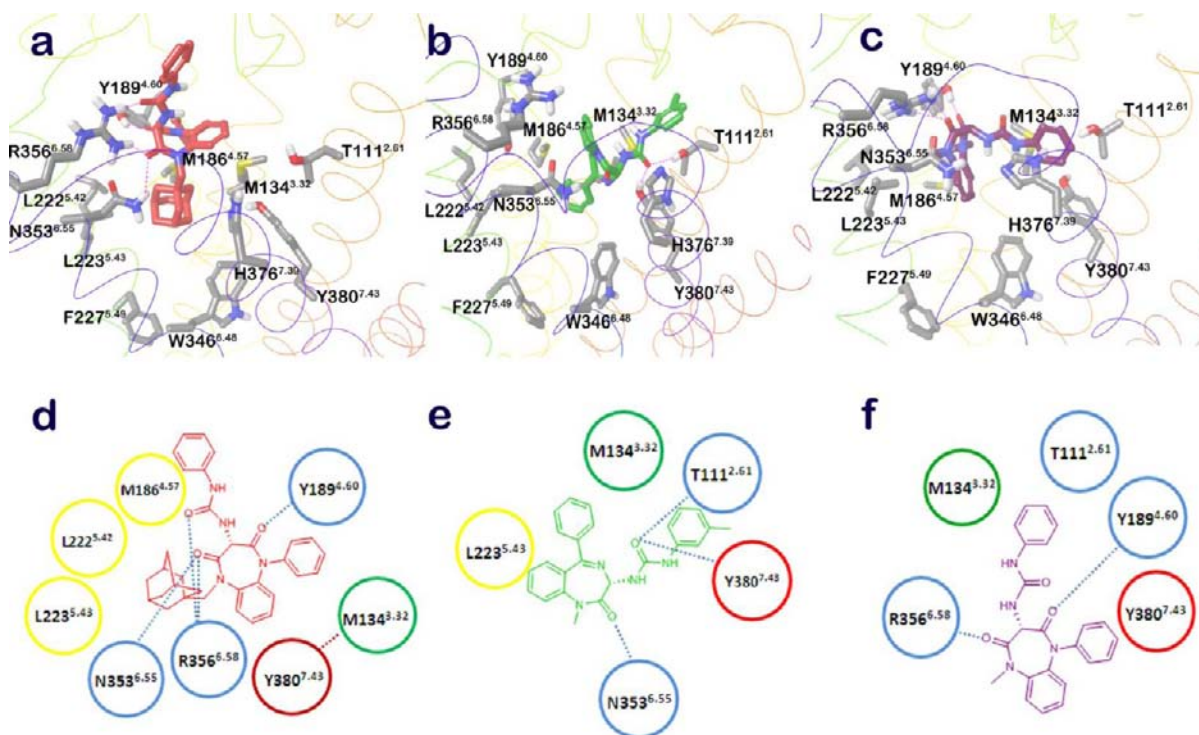


Figure 6. Docking poses of benzodiazepine-like antagonists in the modeled CCK2R structure. Binding sites of (a) GV150013X, (b) L365260, and (c) GV-CH3 are shown with the backbone of CCK2R in a curved line and the side chains of the amino acids forming the binding site in stick. The details of docking procedure are given in the Experimental Procedures. The schematic representation of the interactions within the binding site, with highlighted hydrogen bonds, is depicted on corresponding panels d, e, and f. On these panels, residues forming hydrogen bonds are in blue circles, residues forming the hydrophobic pocket are in yellow circles, and residues contributing to stabilization of the CCK2R $^{\beta}$ state are shown in superscript.

is accompanied by changes in the structure of the orthosteric binding pocket.

Proximity of Met134^{3.32} and Tyr380^{7.43} Is Pivotal for Stabilization of the CCK2R $^{\beta}$ State Recruiting β -arrestin-2. The experimental data above suggest that the orthosteric binding site of the CCK2R, which is composed of amino acids from transmembrane helices, display structural differences in the CCK2R $^{\beta}$ state versus the CCK2R G state. We further investigated whether residues from transmembrane helices could be differentially involved in the stability of CCK2R $^{\beta}$ and CCK2R G states. We focused our attention on M134^{3.32}–Y380^{7.43} interactions. Indeed, in the 3D-homology model of the CCK2R G state, the C α atoms of M134^{3.32} and Y380^{7.43} are at a distance of 10 Å and the sulfur atom of M134^{3.32} and the center of aromatic ring of Y380^{7.43} are at a distance of 6.5 Å (Supplementary Fig. 2). We predicted that M134^{3.32} can interact with Y380^{7.43} through a S–HO hydrogen bond or a sulfur–aromatic interaction in the CCK2R $^{\beta}$ state, and this interaction could contribute to stabilization of this state recruiting β -arrestin-2. We tested this hypothesis by constructing several mutants affecting positions 3.32 and 7.43 in the CCK2R.

Confocal microscopy quantification of β -arrestin-2-YFP recruitment to activated CCK2R mutants labeled with Alexa F 647-CCK (Figure 8 and Supplementary Fig. 7) showed that M134A^{3.32} and Y380A^{7.43} mutants poorly recruited β -arrestin-2-YFP relative to the wild-type CCK2R (85 and 55% decreases, respectively, Figure 8e). Correspondingly, mutants M134A^{3.32} and Y380A^{7.43} exhibited dramatic decreases in the maximal net BRET signal relative to the wild-type CCK2R (75 and 45% decreases, respectively) (Figure 8g). These maximum BRET decreases were confirmed by titration curves of M134A^{3.32} and

Y380A^{7.43} mutants in the presence of saturated levels of β -arrestin-2-YFP (Supplementary Fig. 8).

Remarkably, M134A^{3.32} and Y380A^{7.43} mutants responded to CCK-induced production of inositol phosphates with the same efficacy as the wild-type CCK2R (Figure 8h). A shift of potency reflecting contribution of residue Y380A^{7.43} to CCK binding affinity²⁹ was, however, observed with both inositol phosphate production and BRET dose–response curves. Control experiments indicated that expression levels of the mutants were similar to the wild-type CCK2R (Supplementary Fig. 9). Therefore, the two amino acids, M134^{3.32} and Y380^{7.43} appear to be much more involved in efficacy of CCK-stimulated β -arrestin-2 recruitment to the CCK2R than in efficacy of phospholipase-C stimulation.

Additional mutants were constructed to study the interaction between M134^{3.32} and Y380^{7.43} and its role in CCK2R $^{\beta}$ state stabilization. The possibility of H-bond interaction between M134^{3.32} and Y380^{7.43} was first explored. BRET results (Supplementary Fig. 10), show that mutant Y380F^{7.43} recruited β -arrestin-2 similarly to the wild-type CCK2R ruling out the possibility of H-bond interaction between M134^{3.32} and Y380^{7.43}. On the other hand, mutant M134C^{3.32} showed high basal BRET in the presence of β -arrestin-2-YFP relative to the wild-type CCK2R, suggesting a constitutive recruitment of β -arrestin-2-YFP (Figure 8g). However, with this mutant, BRET signal could not be increased upon CCK stimulation. In fact, confocal microscopy observation of cells expressing the mutant M134^{3.32}C indicated that it was not detected at the cell surface but was present in numerous intracellular vesicles containing β -arrestin-2-YFP (Figure 8f). As expected, this mutant did not exhibit inositol phosphate production (Figure 8h). Thus, to

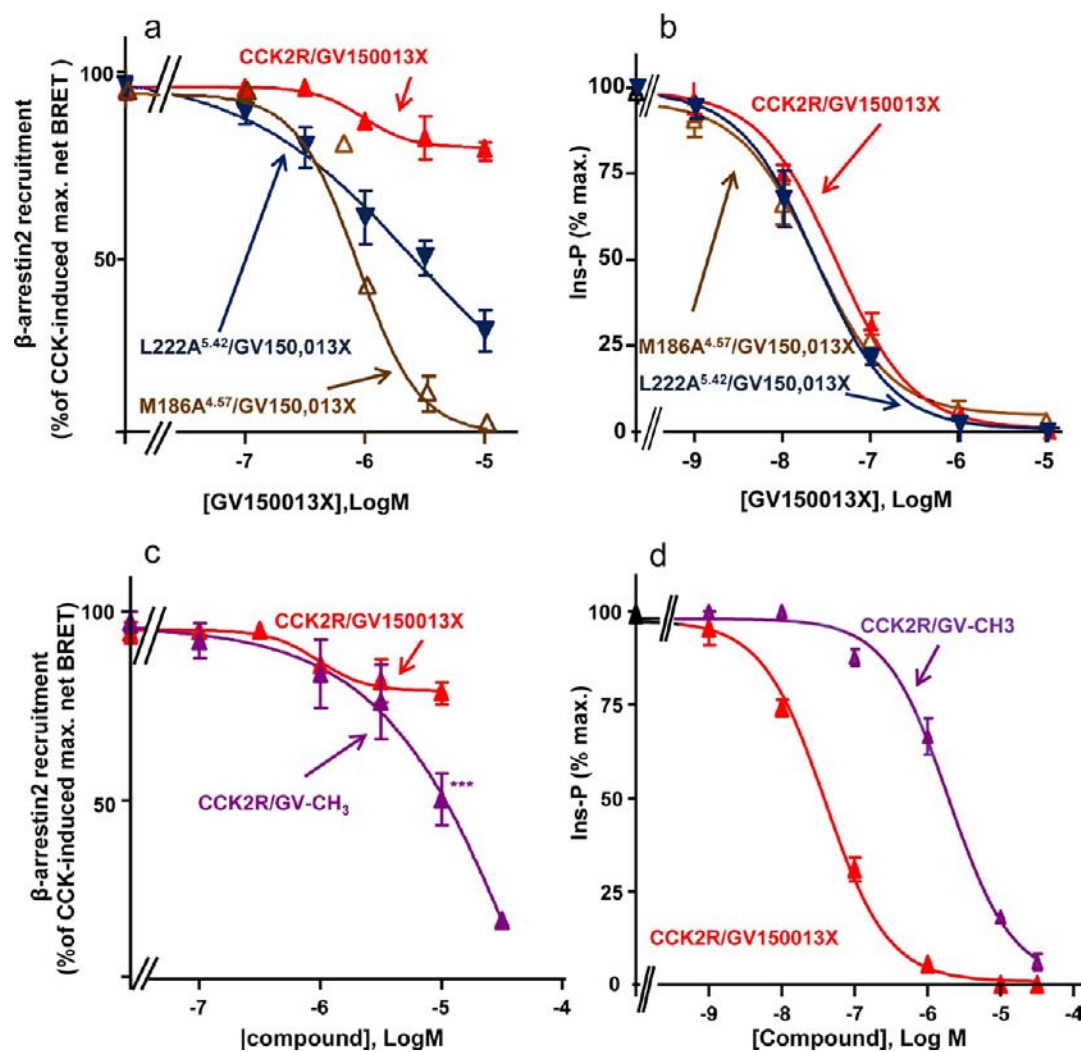


Figure 7. Mutations within orthosteric binding site of CCK2R or substitution of adamantane group by methyl in GV150013X restore antagonist activity on CCK2R^β state. M186^{4.57} or L222^{5.42} of CCK2R, potentially in contact with the bulky adamantane group of GV150013X when docked in the binding site of modeled CCK2R^G (Figure 6a), were mutated to alanine. (a) Mutations M186A^{4.57} and L222A^{5.42} restore the ability of GV150013X to inhibit BRET between β -arrestin-2 and CCK2R. (b) In contrast, mutations M186A^{4.57} and L222A^{5.42} have minor effects on the potency of GV150013X on CCK-induced production of inositol phosphates. (c) Substitution of the adamantane group in GV150013X by a methyl group enables the antagonist GV-CH₃ to inhibit BRET between β -arrestin-2 and wild-type CCK2R. (d) In contrast, substitution of the adamantane group in GV150013X by a methyl group dramatically decreases the potency of the antagonist to inhibit CCK-induced inositol phosphate production. Experiments were carried out as for Figure 2. Values of IC₅₀ (corresponding to potency) are reported in Table 2. Note that due to solubility limits in the incubation medium, GV150013X could not be tested at concentrations higher than 10 μ M.

Table 2. Effects of Adamantane Substitution in GV150013X and M186A^{4.57} or L222A^{5.42} Mutations in CCK2R on the Potency of the Antagonist on CCK2R^β State Recruiting β -Arrestins or CCK2R^G State Activating Phospholipase-C^a

	IC ₅₀ ± SEM (nM)			
	CCK-induced β -arrestin-2 recruitment		CCK-induced PLC activation	
	GV150013X	GV-CH ₃	GV150013X	GV-CH ₃
WT	NC	13500 ± 4300	39.9 ± 5.4	1958 ± 440
M186A ^{4.57}	300 ± 60	230 ± 80	25.8 ± 9.2	2260 ± 730
L222A ^{5.42}	~2500	800 ± 200	23.2 ± 7.2	2710 ± 520

^aCCK2R^β recruiting β -arrestins and CCK2R^G state activating phospholipase-C were monitored by BRET and inositol phosphate measurement, respectively. Results are given as IC₅₀ (potency), corresponding to concentrations of antagonists inhibiting half of CCK(10 nM)-induced responses. Dose–response curves for both biological assays are given in Figure 7 and Supplementary Fig. 4. Values are mean ± SEM of three separate experiments. NC = value cannot be calculated.

summarize, modeling predictions validated by experimental results with M134A^{3.32} and Y380A^{7.43} mutants support the hypothesis that the interaction between M134^{3.32} and Y380^{7.43} is

required for the CCK-induced CCK2R^β state recruiting β -arrestin-2. Furthermore, normal recruitment of β -arrestin-2 by Y380F^{7.43} together with high level recruitment of β -arrestin-2 by

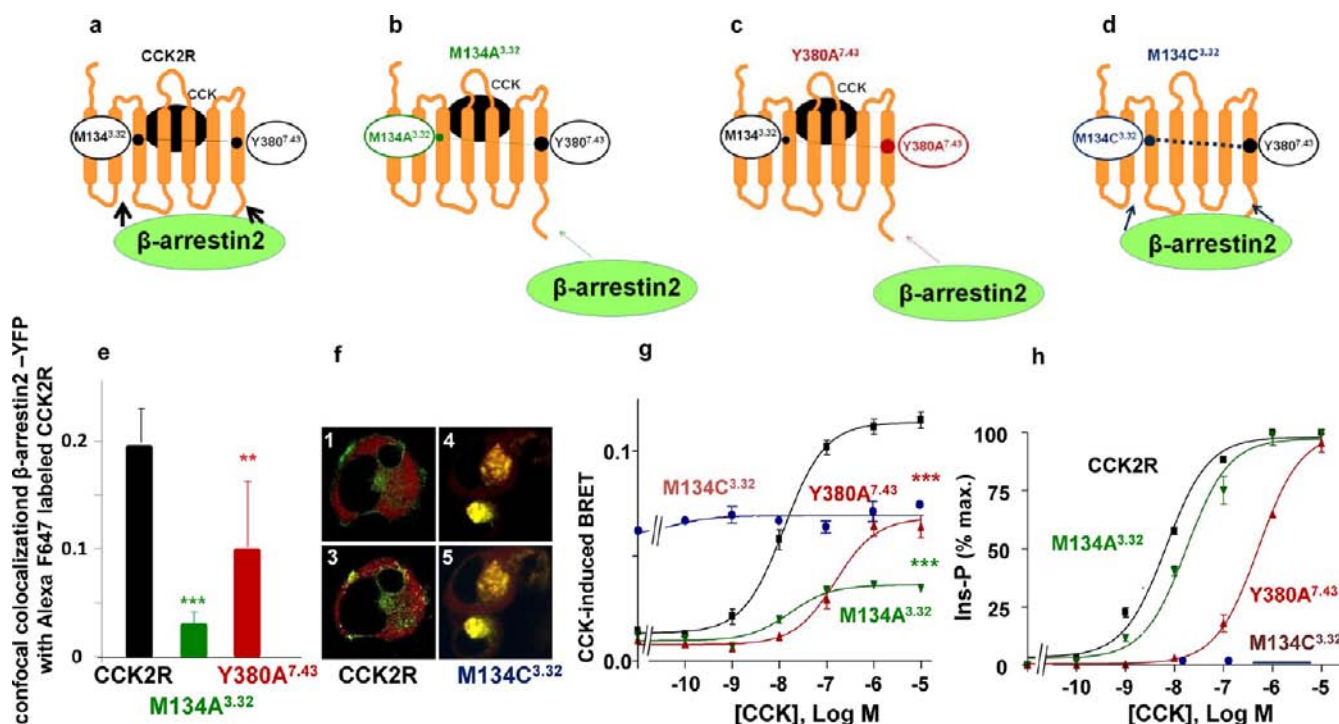


Figure 8. M134^{3.32} and Y380^{7.43} in the CCK2R are differently involved in the stabilization of the CCK2R^β state recruiting β-arrestin-2 or the CCK2R^G state stimulating phospholipase-C. (a–d) Schematic representation of β-arrestin-2 recruitment to wild-type and mutated CCK2R at positions M134^{3.32} and Y380^{7.43}. (e) Confocal microscopy analyses showing that mutation M134A^{3.32} or Y380A^{7.43} decreased by 85% or 55% recruitment of β-arrestin-2 to CCK2R, respectively. (f) Confocal microscopy image showing (1) absence of co-localization between CCK2R-GFP (in green) and β-arrestin-2-RFP (in red) before CCK stimulation; (2) recruitment of β-arrestin-2-RFP to CCK2R-GFP (yellow spots) upon CCK stimulation (20 min, 10 nM CCK); and (3) intracellular co-localization of M134C^{3.32}-GFP and β-arrestin-2-RFP (yellow) in the absence of CCK or (4) in the presence of CCK. (g) BRET dose–response curves showing decreases of 75 or 45% of maximal CCK-induced BRET signal between β-arrestin-2 and M134A^{3.32} or Y380A^{7.43} mutants as well as high basal BRET signal between β-arrestin-2 and M134C^{3.32}. (h) Dose–response curves for inositol phosphate production showing absence of effect of mutations M134A^{3.32} or Y380A^{7.43} on maximal CCK-induced phospholipase-C activation. Maximal inositol production with the mutants is expressed as the percent of maximal production achieved with the wild-type CCK2R. Note that shifts in potencies observed for BRET and inositol phosphate curves with mutant Y380A^{7.43} reflect involvement of residue Y380A^{7.43} in interaction with CCK in the binding site.²² Experiments in (e) were carried out with HEK 293T cells coexpressing transiently wild-type or mutated CCK2R and β-arrestin-2-YFP. Recruitment of β-arrestin-2-YFP to activated receptors (labeled by Alexa F 647-CCK) was quantified at 5 min of stimulation as described in the Experimental Procedures. (f) Experiments were carried out with HEK 293T cells coexpressing transiently CCK2R-GFP or M134C^{3.32}-GFP and β-arrestin-2-RFP. (g) Experiments were carried with HEK 293T cells expressing transiently wild-type or mutated CCK2R-Rluc and β-arrestin-2-YFP. (h) Experiments were carried with HEK 293T cells expressing transiently wild-type or mutated CCK2R-Rluc. Asterisks indicate the *p* values giving the significance of β-arrestin-2-YFP recruitment by mutants relative to wild-type CCK2R: ** 0.001 < *p* < 0.01; *** *p* < 0.001.

M134C^{3.32} mutant in the absence of CCK strongly suggest that residue M134^{3.32} or C134^{3.32} and Y380^{7.43} are able to form a sulfur–aromatic interaction that likely holds the receptor in the CCK2R^β state in the presence or in the absence of CCK, respectively.

We have further examined the possibility of sulfur–aromatic interaction conducting the molecular dynamics simulations of our CCK2R model in the ligand free form, occupied with CCK and the ligand free form of M134C^{3.32} mutant. Molecular dynamics simulations represent a theoretical and computational method that uses Newton’s law of motion to predict protein plasticity in interactions and function. The simulation data indicate that the sulfur–aromatic distance between M134^{3.32} and Y380^{7.43} is shorter and more stable with the average value of 4.5 Å in the presence of CCK than in the unoccupied wild-type CCK2R (Figure 9a), suggesting that CCK stabilizes M134^{3.32}–Y380^{7.43} contacts. Notably, our experimentally validated model of an agonist–receptor interactions built in the previous studies^{22,29} suggests that side chains of residue Met/Leu of CCK which are the closest to residues M134^{3.32} and Y380^{7.43} of

the CCK2R (Supplementary Fig. 2), might play as catalyzing role, forcing the side chains of M134^{3.32} and Y380^{7.43} to adopt a favorable conformation to promote sulfur–aromatic interaction. The distance between the aromatic ring and sulfur atom remains short and stable (4 Å) in the simulations of the unoccupied M134C^{3.32} mutant (Figure 9a), suggesting that the Cys–Tyr distance and the polarity of the S–H group can stabilize the sulfur–aromatic interaction in the absence of CCK. In Figure 9b, we show the typical molecular dynamics structures of the wild-type CCK2R and M134C^{3.32} mutant, from which one can see the face position of the Cys and the distant position of Met to the Tyr ring.

DISCUSSION

The newly recognized ability of β-arrestins to serve as signal transducers for 7TMRs and the discovery of β-arrestin or G protein biased ligands represent innovative paradigms in 7TMR signaling with potential therapeutic interest.^{7,35} Here, taking CCK2R as a 7TMR model system which both couples to Gαq and recruits β-arrestins, we provide converging pharmacological

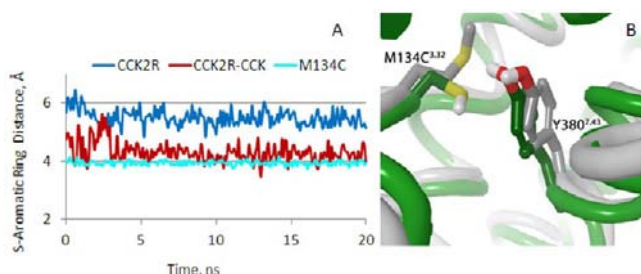


Figure 9. Sulfur–aromatic interactions between residues in position 134^{3.32} and 380^{7.43} in the CCK2R. (a) Time dependence of the distance between S atom of M134^{3.32} and the center of the mass of the aromatic ring of Y380^{7.43} in the unoccupied CCK2R (blue), in the complex CCK2R–CCK (red), and in the unoccupied mutant M134C^{3.32} (cyan) from 20 ns molecular dynamics. The sulfur–aromatic interaction is likely stably present in the CCK2R.CCK complex (4.5 Å), whereas the interaction is poorly seen in the unoccupied CCK2R (>5 Å). In the unoccupied M134C^{3.32} mutant, the distance between the aromatic ring and sulfur atom remains short and constant without needing a ligand. (b) Superimposition of typical molecular dynamics structures of the CCK2R wild-type and M134A^{3.32} mutant. The receptor superimposition is shown from the side view. The backbone of the wild-type and mutant receptor is shown in white and green, respectively, and only the side chains at positions 3.32 and 7.43 are visualized in the stick-like form. The image of the receptor typical structure shows that the sulfur atom of cysteine faces the aromatic ring of Y380^{7.43}, whereas the sulfur of M134^{3.32} is above the aromatic ring of Y380^{7.43}.

and molecular evidence that CCK-induced conformational states of the CCK2R recruiting β -arrestin-2 (termed CCK2R ^{β} state) and that activating phospholipase-C through *G* α q coupling (termed CCK2R^{*G*} state) are distinct. Differences were shown at the CCK2R orthosteric binding site formed by transmembrane helices of the CCK2R. This is of prime importance since biased agonism initiates at the binding site of receptors. Our conclusion is based on strong converging pharmacological and molecular data. First, BRET results, which account for β -arrestin-2 recruitment to the CCK2R showed that CCK-induced formation of CCK2R ^{β} state is competitively inhibited by the two structurally unrelated molecules PD135158 and L365260 but not by GV150013X, whereas CCK-stimulation of CCK2R^{*G*} state is competitively inhibited by the three molecules. In agreement with these results, GV150013X is almost inefficient to competitively block CCK-induced CCK2R internalization, a process, which was previously demonstrated to involve β -arrestin-2 recruitment.²³ Second, CCK2R binding sites presenting a low affinity for CCK and to which GV150013X is unable to compete efficiently with CCK were identified in addition to high affinity CCK binding sites which can bind GV150013X with a high affinity. The low affinity CCK binding sites likely corresponded to CCK2R ^{β} state recruiting β -arrestin2.

Furthermore, our attempts at using structural modeling and site-directed mutagenesis to identify structural elements which most likely hinder binding of GV150013X to CCK-induced CCK2R ^{β} state showed that two mutations within the orthosteric binding site of CCK2R (M186A^{4.57} or L222A^{5.42}) or substitution of adamantane group by methyl in GV150013X restores part of the antagonist activity on the CCK2R ^{β} state, whereas these mutations or chemical substitution cause either minor effects or dramatic decreases on antagonist potency on CCK-induced formation of CCK2R^{*G*}, respectively. All together the data strongly support that the shape of the orthosteric

binding cavity of the CCK2R, which is composed of residues from transmembrane helices, is modified in the CCK2R ^{β} state relative to the CCK2R^{*G*} state. Third, mutation of two interacting amino acids from helices 3 and 7, namely M134^{3.32} and Y380^{7.43} produced CCK2R variants, which either poorly recruit β -arrestin-2 after CCK stimulation or recruit β -arrestin-2 in the absence of CCK.

The key role of M134^{3.32}–Y380^{7.43} interaction in the stability of the CCK2R ^{β} state through S–aromatic interaction, and possible changes in relative position and/or orientation of helix 3 and 7 are in line with reports that associate conformational changes in helix 7 of the β_2 -adrenergic receptor and β -arrestin-biased agonists stimulation.^{13,15} Interestingly, interaction between M134^{3.32} and Y380^{7.43} is observed in CCK2R ^{β} state recruiting β -arrestin-2 while an equivalent constraint is found in most crystallized members of class A 7TMRs at the level of the ligand binding pocket.^{11,15,25,36–48} The nature of this constraint and its role in the stabilization of different signaling conformations would have evolved in different sub-families. Indeed, M134^{3.32}–Y380^{7.43} interaction in CCK2R corresponds to the D^{3.32}–Y^{7.43} hydrogen bond in aminergic receptors (<http://lmc.uab.cat/gmos>). Furthermore, in aminergic receptors, like in CCK2R, ligands bind very close to these residues and presumably regulate contacts between helices 3 and 7. The existence of S–aromatic interactions is well documented in several proteins,^{49,50} but rarely in 7TMRs. However, analysis of crystal structures revealed that S–aromatic contacts occur much more frequently than would be expected from random association.⁵¹ Estimates for the S–aromatic interaction energies give comparable values to aromatic–aromatic interactions or N–H...O hydrogen bonds.^{49,52}

Although the current study does not provide 3-D structures of CCK2R ^{β} and CCK2R^{*G*} states, it is foreseeable that differences at the binding site level and the relative position of helices 3 and 7 are accompanied by conformational changes in intracellular parts of the receptor. The specific structural changes and mechanism remain to be identified. As a second major predictable structural difference, CCK2R is likely phosphorylated at specific positions in the CCK2R ^{β} state, but not in the CCK2R^{*G*} state, since the phosphorylation by GRK is subsequent to activation of G protein-dependent signals.⁵ However, we previously showed that phosphorylation of the C-terminal region in the CCK2R upon CCK stimulation favors β -arrestin-2 recruitment, but is dispensable.²³ Hence, binding of β -arrestin-2 to CCK2R ^{β} state compulsorily involves other regions of the receptor (most likely intracellular parts), the conformation of which should be different in CCK2R ^{β} state relative to CCK2R^{*G*} state. This view agrees with the accepted mechanism of recognition between 7TMRs and arrestins involving two main sites of interaction on both partners, which were termed “activation-recognition” and “phosphorylation-recognition” sites.^{53,54} The phosphorylation-recognition site of arrestins discriminates phosphorylated from unphosphorylated 7TMRs. So, this phosphorylation-recognition is unable to select a particular 7TMR.^{55,56} The activation-recognition site in arrestins discriminates active from inactive 7TMRs and interaction through this site seems to be sufficient for activation of arrestins. Indeed, phosphorylation-deficient mutants of 7TMRs were shown to cause similar conformational changes in β -arrestin-2 as the wild-type corresponding 7TMRs.⁵⁷

How changes identified in the CCK2R ^{β} state versus CCK2R^{*G*} state occur is an unresolved issue. However, as we previously simulated for transition from inactive CCK2R to CCK2R^{*G*},¹⁹ it

is predictable that coordinated motions of helices involving several networks of interactions cause changes within the binding cavity, which propagate to intracellular portions of the receptor forming binding site of β -arrestin-2. It is also plausible that binding of β -arrestin-2 to the phosphorylated region of CCK2R and subsequently to the activation-recognition site contributes to formation and stabilization of the CCK2R $^{\beta}$ state. Hence, the fact that the CCK2R $^{\beta}$ state appears to be stabilized by slightly higher concentrations of CCK than does the CCK2R $^{\text{G}}$ state might result in part from β -arrestin binding which, as an allosteric regulator transmits conformational changes to the orthosteric binding site. This view is in line with structural and pharmacological data whereby binding affinity of agonists for 7TMR, including CCK receptors, is augmented by heterotrimeric G protein coupling, which, therefore, acts as allosteric regulators on the binding site.^{9,58} It is worthy to note that changes in the position of some residues in the orthosteric binding site of CCK2R $^{\beta}$ state relative to CCK2R $^{\text{G}}$ state hinder binding of the non-peptide antagonist GV150013X whereas these changes less significantly affect CCK recognition. This observation is in line with data showing that a synthetic ligand can be sensitive to minor changes within the orthosteric binding site of a 7TMR whereas the natural agonist is not or is less sensitive to such changes. For instance, canine and human CCK2R recognize CCK with strictly identical affinities but display very different affinities toward a synthetic antagonist. The presence of a val in helice VI in canine CCK2R and Ile at the same position in human CCK2R (so two residues with very similar side-chains) explains the different pharmacological behaviors.⁵⁹ At last, the existence of CCK2R $^{\beta}$ state distinct from CCK2R $^{\text{G}}$ state must be discussed in light of accumulating data indicating that 7TMRs can exist both as monomer, homodimers or larger oligomeric forms functionally selective in the cell surface membrane.^{60–62} Thus, it is not excluded that CCK2R $^{\beta}$ and CCK2R $^{\text{G}}$ states correspond to distinct structural entities. An agonist dose-dependent switch from G protein-coupled to G protein-independent signaling was previously reported for β_2 -adrenergic receptor.⁶³ Indeed, β_2 -adrenergic receptor signals through G α_s upon low concentrations of agonist to activate MAP kinase pathway, whereas it signals also via a Src-dependent G protein-independent pathway upon higher agonist concentrations. The authors proposed a mechanism whereby high concentrations of agonists stabilize dimers of β_2 -adrenergic receptor, providing structural features necessary for direct activation of Src by bringing two molecules of Src into proximity, and allowing their intermolecular autophosphorylation and activation.⁶³

Two major consequences of our findings can be anticipated regarding the CCK2R. First, since GV150013X is not able to inhibit CCK-induced recruitment of β -arrestin-2, this compound should not be able to efficiently block CCK2R-induced β -arrestin-2-dependent signaling pathways and associated events, as illustrated with CCK2R internalization. This might be of high importance owing to expression of the CCK2R in a large variety of cancers and its recognized contribution to tumoral progression as well as increasing role of β -arrestin1/2-dependent signaling pathways to cancer progression.^{35,64–66} Second, determination of the structure of CCK2R both in the CCK2R $^{\beta}$ and CCK2R $^{\text{G}}$ states is required to enable design of new ligands of desired pharmacological profiles. In particular, a β -arrestin1/2-biased CCK2R agonist, would be very helpful to delineate consequences of new signaling pathways downstream of the CCK2R in cellular and animal models of cancer.

CONCLUSION

This study provides converging pharmacological and molecular evidence that a 7TMR, the CCK2R, can adopt distinct conformations to either trigger G protein signaling or β -arrestin-2 recruitment. These conformations are distinguishable at the orthosteric binding site which is defined by transmembrane helices. An antagonist of the CCK2R, GV150013X, was identified as a biased antagonist on β -arrestin-2 recruitment pathway. Two interacting amino acids, M^{3,32} and Y^{7,43}, play key roles in formation/stabilization of a state recruiting or β -arrestin-2. These findings shall have future impact not only on CCK2R pharmacology but also on 7TMRs in general, and they validate the relevance of the design of biased ligands able to selectively target each functional conformation of 7TMRs.

ASSOCIATED CONTENT

Supporting Information

Supplementary figures, legends to those figures, and supplementary methods. This material is available free of charge via the Internet at <http://pubs.acs.org>.

AUTHOR INFORMATION

Corresponding Author

daniel.fourmy@inserm.fr; i.tikhonova@qub.ac.uk

Notes

The authors declare no competing financial interest.

ACKNOWLEDGMENTS

We greatly appreciate the gifts of plasmids encoding YFP-tagged β -arrestin-2 from Marc Caron (Duke University Medical Center) and GFP-tagged β -arrestin-2 from Robert Lefkowitz (Duke University Medical Center). We thank Dr Romina D'Angelo from Cellular Imaging Facility Rangueil (I2MC/TRI Platform) for excellent technical support and advice on confocal microscopy and image analysis, and Chantal Zedde and Isabelle Fabing (CNRS, LSPCMIB, UMR-5068) for purification of GV-CH3. The work was supported by Grants from Association pour la Recherche contre le Cancer (ARC No. 4870) and Ligue Nationale Contre le Cancer (comité 31). A.C. is supported by a grant from Instituto de Salud Carlos III.

REFERENCES

- (1) Hopkins, A. L.; Groom, C. R. *Nat. Rev. Drug Discov.* **2002**, *1*, 727.
- (2) Rajagopal, S.; Rajagopal, K.; Lefkowitz, R. J. *Nat. Rev. Drug Discov.* **2010**, *9*, 373.
- (3) Lefkowitz, R. J.; Shenoy, S. K. *Science* **2005**, *308*, 512.
- (4) DeFea, K. A. *Cell Signal.* **2011**, *23*, 621.
- (5) Ferguson, S. S. *Pharmacol. Rev.* **2001**, *53*, 1.
- (6) Hanyaloglu, A. C.; von Zastrow, M. *Annu. Rev. Pharmacol. Toxicol.* **2008**, *48*, 537.
- (7) Whalen, E. J.; Rajagopal, S.; Lefkowitz, R. J. *Trends Mol. Med.* **2011**, *17*, 126.
- (8) Vaidehi, N.; Kenakin, T. *Curr. Opin. Pharmacol.* **2010**, *10*, 775.
- (9) Rasmussen, S. G.; DeVree, B. T.; Zou, Y.; Kruse, A. C.; Chung, K. Y.; Kobilka, T. S.; Thian, F. S.; Chae, P. S.; Pardon, E.; Calinski, D.; Mathiesen, J. M.; Shah, S. T.; Lyons, J. A.; Caffrey, M.; Gellman, S. H.; Steyaert, J.; Skiniotis, G.; Weis, W. I.; Sunahara, R. K.; Kobilka, B. K. *Nature* **2011**, *477*, 549.
- (10) Xu, F.; Wu, H.; Katritch, V.; Han, G. W.; Jacobson, K. A.; Gao, Z. G.; Cherezov, V.; Stevens, R. C. *Science* **2011**, *332*, 322.
- (11) Lebon, G.; Warne, T.; Edwards, P. C.; Bennett, K.; Langmead, C. J.; Leslie, A. G.; Tate, C. G. *Nature* **2011**, *474*, 521.

- (12) Warne, T.; Moukhametzianov, R.; Baker, J. G.; Nehme, R.; Edwards, P. C.; Leslie, A. G.; Schertler, G. F.; Tate, C. G. *Nature* **2011**, *469*, 241.
- (13) Granier, S.; Kim, S.; Shafer, A. M.; Ratnala, V. R.; Fung, J. J.; Zare, R. N.; Kobilka, B. *J. Biol. Chem.* **2007**, *282*, 13895.
- (14) Kahsai, A. W.; Xiao, K.; Rajagopal, S.; Ahn, S.; Shukla, A. K.; Sun, J.; Oas, T. G.; Lefkowitz, R. J. *Nat. Chem. Biol.* **2011**, *7*, 692.
- (15) Liu, J. J.; Horst, R.; Katritch, V.; Stevens, R. C.; Wuthrich, K. *Science* **2012**, *335*, 1106.
- (16) Rahmeh, R.; Damian, M.; Cottet, M.; Orcel, H.; Mendre, C.; Durroux, T.; Sharma, K. S.; Durand, G.; Pucci, B.; Trinquet, E.; Zwier, J. M.; Deupi, X.; Bron, P.; Baneres, J. L.; Mouillac, B.; Granier, S. *Proc. Natl. Acad. Sci. U.S.A.* **2012**, *109*, 6733.
- (17) Dufresne, M.; Seva, C.; Fourmy, D. *Physiol. Rev.* **2006**, *86*, 805.
- (18) Yaqub, T.; Tikhonova, I. G.; Lattig, J.; Magnan, R.; Laval, M.; Escrieut, C.; Boulegue, C.; Hewage, C.; Fourmy, D. *Mol. Pharmacol.* **2010**, *77*, 547.
- (19) Hughes, J.; Boden, P.; Costall, B.; Domeney, A.; Kelly, E.; Horwell, D. C.; Hunter, J. C.; Pinnock, R. D.; Woodruff, G. N. *Proc. Natl. Acad. Sci. U.S.A.* **1990**, *87*, 6728.
- (20) Bock, M. G.; DiPardo, R. M.; Evans, B. E.; Rittle, K. E.; Whitter, W. L.; Veber, D. E.; Anderson, P. S.; Freidinger, R. M. *J. Med. Chem.* **1989**, *32*, 13.
- (21) Ursini, A.; Capelli, A. M.; Carr, R. A.; Cassara, P.; Corsi, M.; Curcuruto, O.; Curotto, G.; Dal Cin, M.; Davalli, S.; Donati, D.; Feriani, A.; Finch, H.; Finizia, G.; Gaviraghi, G.; Marien, M.; Pentassuglia, G.; Polinelli, S.; Ratti, E.; Reggiani, A. M.; Tarzia, G.; Tedesco, G.; Tranquillini, M. E.; Trist, D. G.; Van Amsterdam, F. T. *J. Med. Chem.* **2000**, *43*, 3596.
- (22) Foucaud, M.; Marco, E.; Escrieut, C.; Low, C.; Kalindjian, B.; Fourmy, D. *J. Biol. Chem.* **2008**, *283*, 35860.
- (23) Magnan, R.; Masri, B.; Escrieut, C.; Foucaud, M.; Cordelier, P.; Fourmy, D. *J. Biol. Chem.* **2011**, *286*, 6707.
- (24) Masri, B.; Salahpour, A.; Didriksen, M.; Ghisi, V.; Beaulieu, J. M.; Gainetdinov, R. R.; Caron, M. G. *Proc. Natl. Acad. Sci. U.S.A.* **2008**, *105*, 13656.
- (25) Rasmussen, S. G.; Choi, H. J.; Fung, J. J.; Pardon, E.; Casarosa, P.; Chae, P. S.; Devree, B. T.; Rosenbaum, D. M.; Thian, F. S.; Kobilka, T. S.; Schnapp, A.; Konetzki, I.; Sunahara, R. K.; Gellman, S. H.; Pautsch, A.; Steyaert, J.; Weis, W. I.; Kobilka, B. K. *Nature* **2011**, *469*, 175.
- (26) Gales, C.; Poirot, M.; Taillefer, J.; Maigret, B.; Martinez, J.; Moroder, L.; Escrieut, C.; Pradayrol, L.; Fourmy, D.; Silvente-Poirot, S. *Mol. Pharmacol.* **2003**, *63*, 973.
- (27) Silvente-Poirot, S.; Escrieut, C.; Gales, C.; Fehrentz, J. A.; Escherich, A.; Wank, S. A.; Martinez, J.; Moroder, L.; Maigret, B.; Bouisson, M.; Vaysse, N.; Fourmy, D. *J. Biol. Chem.* **1999**, *274*, 23191.
- (28) Foucaud, M.; Archer-Lahlou, E.; Marco, E.; Tikhonova, I. G.; Maigret, B.; Escrieut, C.; Langer, I.; Fourmy, D. *Regul. Pept.* **2008**, *145*, 17.
- (29) Marco, E.; Foucaud, M.; Langer, I.; Escrieut, C.; Tikhonova, I. G.; Fourmy, D. *J. Biol. Chem.* **2007**, *282*, 28779.
- (30) Tikhonova, I. G.; Marco, E.; Lahlou-Archer, E.; Langer, I.; Foucaud, M.; Maigret, B.; Fourmy, D. *Curr. Top. Med. Chem.* **2007**, *7*, 1243.
- (31) Langer, I.; Tikhonova, I. G.; Travers, M. A.; Archer-Lahlou, E.; Escrieut, C.; Maigret, B.; Fourmy, D. *J. Biol. Chem.* **2005**, *280*, 22198.
- (32) Sherman, W.; Day, T.; Jacobson, M. P.; Friesner, R. A.; Farid, R. *J. Med. Chem.* **2006**, *49*, 534.
- (33) Humphrey, W.; Dalke, A.; Schulten, K. *J. Mol. Graph.* **1996**, *14*, 27.
- (34) Gales, C.; Kowalski-Chauvel, A.; Dufour, M. N.; Seva, C.; Moroder, L.; Pradayrol, L.; Vaysse, N.; Fourmy, D.; Silvente-Poirot, S. *J. Biol. Chem.* **2000**, *275*, 17321.
- (35) Luttrell, L. M.; Gesty-Palmer, D. *Pharmacol. Rev.* **2010**, *62*, 305.
- (36) Cherezov, V.; Rosenbaum, D. M.; Hanson, M. A.; Rasmussen, S. G.; Thian, F. S.; Kobilka, T. S.; Choi, H. J.; Kuhn, P.; Weis, W. I.; Kobilka, B. K.; Stevens, R. C. *Science* **2007**, *318*, 1258.
- (37) Chien, E. Y.; Liu, W.; Zhao, Q.; Katritch, V.; Han, G. W.; Hanson, M. A.; Shi, L.; Newman, A. H.; Javitch, J. A.; Cherezov, V.; Stevens, R. C. *Science* **2011**, *330*, 1091.
- (38) Choe, H. W.; Kim, Y. J.; Park, J. H.; Morizumi, T.; Pai, E. F.; Krauss, N.; Hofmann, K. P.; Scheerer, P.; Ernst, O. P. *Nature* **2011**, *471*, 651.
- (39) Granier, S.; Manglik, A.; Kruse, A. C.; Kobilka, T. S.; Thian, F. S.; Weis, W. I.; Kobilka, B. K. *Nature* **2012**, *485*, 400.
- (40) Haga, K.; Kruse, A. C.; Asada, H.; Yurugi-Kobayashi, T.; Shiroishi, M.; Zhang, C.; Weis, W. I.; Okada, T.; Kobilka, B. K.; Haga, T.; Kobayashi, T. *Nature* **2012**, *482*, 547.
- (41) Hanson, M. A.; Roth, C. B.; Jo, E.; Griffith, M. T.; Scott, F. L.; Reinhart, G.; Desale, H.; Clemons, B.; Cahalan, S. M.; Schuerer, S. C.; Sanna, M. G.; Han, G. W.; Kuhn, P.; Rosen, H.; Stevens, R. C. *Science* **2012**, *335*, 851.
- (42) Jaakola, V. P.; Griffith, M. T.; Hanson, M. A.; Cherezov, V.; Chien, E. Y.; Lane, J. R.; Ijzerman, A. P.; Stevens, R. C. *Science* **2008**, *322*, 1211.
- (43) Murakami, M.; Kouyama, T. *Nature* **2008**, *453*, 363.
- (44) Shimamura, T.; Shiroishi, M.; Weyand, S.; Tsujimoto, H.; Winter, G.; Katritch, V.; Abagyan, R.; Cherezov, V.; Liu, W.; Han, G. W.; Kobayashi, T.; Stevens, R. C.; Iwata, S. *Nature* **2011**, *475*, 65.
- (45) Thompson, A. A.; Liu, W.; Chun, E.; Katritch, V.; Wu, H.; Vardy, E.; Huang, X. P.; Trapella, C.; Guerrini, R.; Calo, G.; Roth, B. L.; Cherezov, V.; Stevens, R. C. *Nature* **2012**, *485*, 395.
- (46) Warne, T.; Serrano-Vega, M. J.; Baker, J. G.; Moukhametzianov, R.; Edwards, P. C.; Henderson, R.; Leslie, A. G.; Tate, C. G.; Schertler, G. F. *Nature* **2008**, *454*, 486.
- (47) Wu, B.; Chien, E. Y.; Mol, C. D.; Fenalti, G.; Liu, W.; Katritch, V.; Abagyan, R.; Brooun, A.; Wells, P.; Bi, F. C.; Hamel, D. J.; Kuhn, P.; Handel, T. M.; Cherezov, V.; Stevens, R. C. *Science* **2010**, *330*, 1066.
- (48) Manglik, A.; Kruse, A. C.; Kobilka, T. S.; Thian, F. S.; Mathiesen, J. M.; Sunahara, R. K.; Pardo, L.; Weis, W. I.; Kobilka, B. K.; Granier, S. *Nature* **2012**, *485*, 321.
- (49) Meyer, E. A.; Castellano, R. K.; Diederich, F. *Angew. Chem., Int. Ed.* **2003**, *42*, 1210.
- (50) Chakrabarti, P.; Bhattacharyya, R. *Prog. Biophys. Mol. Biol.* **2007**, *95*, 83.
- (51) Zauhar, R. J.; Colbert, C. L.; Morgan, R. S.; Welsh, W. J. *Biopolymers* **2000**, *53*, 233.
- (52) Ringer, A. L.; Senenko, A.; Sherrill, C. D. *Protein Sci.* **2007**, *16*, 2216.
- (53) Gurevich, V. V.; Gurevich, E. V. *Trends Pharmacol. Sci.* **2004**, *25*, 105.
- (54) Gurevich, V. V.; Gurevich, E. V. *Pharmacol. Ther.* **2006**, *110*, 465.
- (55) Vishnivetskiy, S. A.; Gimenez, L. E.; Francis, D. J.; Hanson, S. M.; Hubbell, W. L.; Klug, C. S.; Gurevich, V. V. *J. Biol. Chem.* **2011**, *286*, 24288.
- (56) Zhan, X.; Gimenez, L. E.; Gurevich, V. V.; Spiller, B. W. *J. Mol. Biol.* **2011**, *406*, 467.
- (57) Shukla, A. K.; Violin, J. D.; Whalen, E. J.; Gesty-Palmer, D.; Shenoy, S. K.; Lefkowitz, R. J. *Proc. Natl. Acad. Sci. U.S.A.* **2008**, *105*, 9988.
- (58) Huang, S. C.; Fortune, K. P.; Wank, S. A.; Kopin, A. S.; Gardner, J. D. *J. Biol. Chem.* **1994**, *269*, 26121.
- (59) Beinborn, M.; Lee, Y. M.; McBride, E. W.; Quinn, S. M.; Kopin, A. S. *Nature* **1993**, *362*, 348.
- (60) Fung, J. J.; Deupi, X.; Pardo, L.; Yao, X. J.; Velez-Ruiz, G. A.; Devree, B. T.; Sunahara, R. K.; Kobilka, B. K. *EMBO J.* **2009**, *28*, 3315.
- (61) Milligan, G. B. *J. Pharmacol.* **2009**, *158*, 5.
- (62) Urizar, E.; Yano, H.; Kolster, R.; Gales, C.; Lambert, N.; Javitch, J. A. *Nat. Chem. Biol.* **2011**, *7*, 624.
- (63) Sun, Y.; Huang, J.; Xiang, Y.; Bastepe, M.; Juppner, H.; Kobilka, B. K.; Zhang, J. J.; Huang, X. Y. *EMBO J.* **2007**, *26*, 53.
- (64) Watson, S. A.; Grabowska, A. M.; El-Zaatar, M.; Takhar, A. *Nat. Rev. Cancer* **2006**, *6*, 936.

(65) Fourmy, D.; Gigoux, V.; Reubi, J. C. *Gastroenterology* **2011**, *141*, 814.

(66) Gales, C.; Sanchez, D.; Poirot, M.; Pyronnet, S.; Buscal, L.; Cussac, D.; Pradayrol, L.; Fourmy, D.; Silvente-Poirot, S. *Oncogene* **2003**, *22*, 6081.